https://doi.org/10.46813/2024-153-136

DIFFUSION PROCESSES IN METAL LAYERS OF Mo/Si MULTILAYER X-RAY MIRRORS DURING DEPOSITION

Yu.P. Pershyn, V.S. Chumak, A.Yu. Devizenko, E.N. Zubarev, V.A. Sevryukova, N.O. Kyryllova, L.E. Konotopskiy
National Technical University "Kharkiv Polytechnic Institute", Kharkiv, Ukraine
E-mail: pershyny@ukr.net

Small-angle reflectometry, X-ray diffractometry and X-ray tensometry (λ=0.154 nm) were used to study the structure of Mo layers in Mo/Si multilayer X-ray mirrors produced by magnetron sputtering as a function of the Ar pressure in the range of 1…4 mTorr. Two series of samples with periods of about 7 and 14 nm were produced. In all MXMs, Mo layers were crystalline (c-Mo) and Si layers were amorphous. On average, the lattice parameter a_0 in the unstressed state is smaller for the 7 series samples than for the 14 nm series. It increases with Ar pressure, approaching the tabular one. On average, the lattice parameter a_0 in the unstressed state for Mo layers is smaller for the 7 nm series samples than for the 14 nm series. The Si content in the c-Mo layers has been estimated. Diffusion coefficients of silicon atoms into c-Mo layers and their activation energies are determined. Diffusion mechanisms are proposed.

PACS: 61.05.cm, 61.43.Dq, 68.65.Ac, 41.50.+h, 07.85.Fv

INTRODUCTION

Multilayer X-ray mirrors (MXMs) based on a pair of Mo and Si materials have some of the highest reflection coefficients (R>60 %) in the extreme UV region (λ=12.3…18.0 nm) at normal incidence [1–3]. To use them in devices with multimirror arrangement (microscopes, telescopes, lithographs, etc.), in addition to efficiency they should have: a given period distribution over the substrate surface; stable X-ray optical characteristics; low mechanical stresses, etc. In order to satisfy all these requirements together or each point separately, as a first step, it is necessary to characterize as fully as possible the initial structure of the layers, especially Mo-containing layers, since in fact their state ultimately affects most of the mirror characteristics, including efficiency. Controlling the parameters of these layers (thickness, roughness, composition, density, etc.) will help to improve the X-ray optical characteristics of MXMs and bring them closer to the theoretical limit.

Thin Mo layers up to thicknesses of 2…2.6 nm are amorphous (α-Mo) [4–7] due to the excessive content of Si atoms [5, 8]. As the thickness increases, the Mo layers crystallize precisely due to the drop in the Si atom concentration. Data on the composition of Mo layers after crystallization are not considered in the literature.

In as-deposited state, Mo/Si MXMs contain silicide interlayers [8], and their thicknesses at only one interface can reach ~4 nm [9]. The interlayers have an amorphous structure and their nominal composition is close to molybdenum disilicide ($MoSi_2$) [10–12]. The thicknesses of silicide interlayers at different type of interfaces (Si-on-Mo and Mo-on-Si) differ by a factor of ~2 for crystalline Mo (c-Mo) layers [8, 13]. Under external influence (heating, irradiation, etc.) the thicknesses of silicide interlayers grow [13]. For heating and irradiation processes, threshold values at which changes in period and X-ray optical characteristics begin have been established, diffusion coefficients and activation energies of the silicide formation process have been determined [14–16]. However, there is practically no description of the diffusion processes taking place in Mo layers during deposition.

In this work, we estimate the Si atom content in Mo layers in the as-deposited state and analyzed its influence on the X-ray optical properties of Mo/Si MXMs. The diffusion coefficients and activation energies of Si diffusion through the silicide interlayer (Mo-on-Si interface) and redistribution of Si atoms inside Mo layers are determined. The mechanisms responsible for these processes are also proposed.

1. METHODS

The direct-current magnetron sputtering technique was used to deposit the layers. During each experiment, the currents on both magnetrons and the Ar pressure were kept constant to ensure constant deposition rates. However, when the pressure was changed (from 1 to 4 mTorr), even though the magnetron discharge currents were fixed, the deposition rates varied because the sputtering parameters were slightly different (mainly discharge voltages) at each pressure. Component deposition rates dropped from ~0.40 to ~0.36 nm/s for Mo and from ~0.64 to ~0.45 nm/s for Si with pressure and were measured at each specific pressure.

Multilayer X-ray mirrors with periods of 6…16 nm were fabricated by alternate deposition of Mo and Si layers (Mo-layer thickness: $2.3<t_{Mo}<5.9$ nm) from direct-current magnetron sources in Ar atmosphere on flat substrates. Substrates were polished Si wafers and ultra-smooth float glass with RMS surface roughness of 0.3…0.5 nm. Periods of MXMs ranged between 6 and 16 nm. Nominal fraction of Mo-layer thickness in the period was ~0.4. All MXM deposition parameters were controlled by well-calibrated deposition rates. The distance from the magnetron surfaces to the substrate was ~30 mm.

The vacuum chamber was preliminary heated to degas the equipment before applying the layers, and

after cooling down to room temperature, the pressure of residual gases in it did not exceed $2 \cdot 10^{-6}$ Torr.

Small-angle measurements ($2\theta<15°$) to determine an MXM periodicity were performed on an X-ray diffractometer DRON-3M, assembled according to the scheme of a double crystal spectrometer with a (110)Si single crystal as a monochromator. In combination with a 0.1 mm wide slit, this allowed to extract only Cu$K\alpha_1$ line (λ=0.154 nm) from the spectrum produced by the X-ray tube with a copper anode. The beam divergence did not exceed 0.015°. The phase composition of the samples was monitored in the Cu$K\alpha$ radiation on another diffractometer containing a graphite analyzer. The beam divergence in this case was less than 0.5°.

The lattice parameters in the unstressed state were determined by X-ray tensometry ($\sin^2\psi$ method). The smallest errors in determining the lattice parameters are obtained at the largest reflection angles [17]. Therefore, we used the {321} family of planes with diffraction angles at $2\theta \sim 134°$. The shooting of multilayer samples was performed in asymmetric geometry. The calculated values of the angles ψ are given in Table 1.

Table 1

Reflecting planes (hkl) and angles ψ

(hkl)	ψ°	$\sin^2\psi$
(321)	19.1	0.107
(312)	40.9	0.429
(213)	55.5	0.679

For each sample, we took measurements at three different angles. From the angular position of each diffraction maxima, we determined the interplanar distances, lattice periods, and plotted $\sin^2\psi$ plots. Then we determined the values of the lattice parameter a_0 in the unstressed state (at $\sin^2\psi$=0.466).

2. RESULTS AND DISCUSSION

Two series of 10 samples made at successive changes in Ar pressure (p_{Ar}) from 1 to 4 mTorr were studied. The first series consisted of MXMs with periods of (7±1) nm ("7 nm" series), and the second series consisted of mirrors with periods of (14±2) nm ("14 nm" series). We should note that the MXM periods in the first series had close period values for the MXMs used in X-ray lithography. A second series with thicker Mo layers was fabricated to validate the results obtained in the first series, because the thickness of the Mo layers in the first series is close to the amorphization boundary of Mo-layers, and the Mo layers may have too many defects.

2.1. DETERMINATION OF THE LATTICE PARAMETER IN Mo LAYERS

The lattice parameter (a_0) of Mo crystallites in the unstressed state was determined from the analysis of the dependence $a=f(\sin^2\psi)$. An example of the obtained dependence for a sample fabricated at p_{Ar}=2 mTorr is shown in Fig. 1,a. Three experimental points correspond to three angles of the sample inclination (see subsection 1. Methods). The interpolation line (dotted line) drawn through these points allows to determine the lattice parameter a_0 in the unstressed state at $\sin^2\psi=2\nu/(1+\nu)=0.466$ (ν is the Poisson's ratio) [18].

The measured values of the lattice parameters a_0 of Mo crystallites in the unstressed state depending on p_{Ar} are shown in Fig. 1,b. Although the obtained dependences for both series have a similar appearance, but in general, the lattice parameters a_0 (Mo) in the "14 nm" series are larger than that in the "7 nm" series. As it can also be seen from Fig. 1,b, all obtained values of a_0 are lower than the tabulated one (a_0=0.3147 nm). In both short-period and long-period series, the lattice parameter gradually increases, approaching the tabulated value. At the same time, in the long-period series, the lattice parameter grows faster and almost reaches the tabulated value at 4 mTorr.

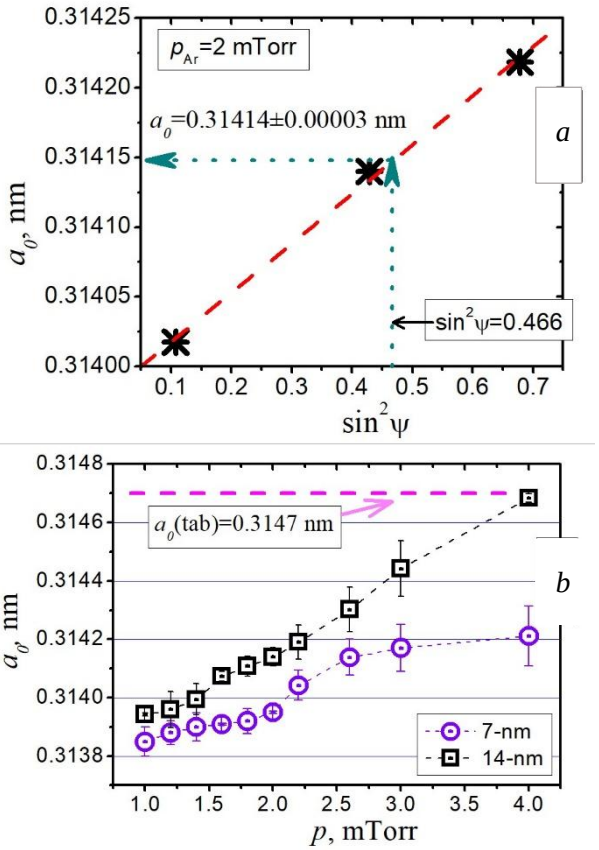

Fig. 1. An example of the $\sin^2\psi$ graph to determine the lattice parameter (a_0) in the unstressed state for Mo crystallites in MXM "14 nm" series fabricated at p_{Ar}=2 mTorr (a). Dependences of a_0 on p_{Ar} for two series of multilayer samples (b)

2.2. ESTIMATION OF IMPURITY CONTENT IN Mo LAYERS

As indicated above, the Mo-crystallite lattice parameters in the unstressed state are lower than the tabulated value (a_0=0.3147 nm). This may be due to the presence of some impurities, for example Si, O, N, C in the Mo layers, since the atomic radii of these elements are smaller than that for Mo (Table 2).

Table 2

Atomic radii of elements

Element	Mo	Si	O	N	C
r, pm	145	110	60	65	70

The reasons for the appearance of impurity atoms in Mo layers can be different. For example, silicon can get into Mo layers from neighboring layers, given that Mo

layers are nanometer thick (t_{Mo}<6 nm). Carbon can enter as hydrocarbons from the diffusion pump oil, nitrogen and oxygen can be in the residual atmosphere of the vacuum chamber. However, the list of impurities can be significantly reduced by detailing the conditions of multilayer deposition. During MXM sputtering we used extremely pure Ar with impurity concentration less than 0.05 %. In order to exclude the presence of residual gases N, O and H_2O in the chamber, the vacuum chamber was heated to 70…100 °C for one hour before the sputtering. This procedure reduced the initial pressure in the vacuum chamber to no more than $2\cdot10^{-3}$ mTorr before sputtering and less than $8\cdot10^{-4}$ mTorr after sputtering. Considering that the working pressure is p_{Ar}~2 mTorr, the concentration of gases in the residual atmosphere during MXM fabrication should not exceed 0.03 %. Since the MXM fabrication was carried out in argon flow, we assume that the concentration of carbon in the deposited layers associated with the counterflow of diffusion oil vapor is also small. In addition, molybdenum and silicon are getters. This is indicated by the decrease in pressure in the vacuum chamber after the fabrication of the samples. Therefore, the deposition of layers in the center of magnetrons was carried out in the zone of reduced content of gas impurities, which were absorbed by the peripheral flow of sputtering substance deposited on the substrate holder.

Previously, we investigated the Mo/Si MXM composition in depth by secondary ion mass spectrometry with sample etching by Ar ions (E_{Ar+}<450 eV) [19]. The MXM periods were ~20 and ~40 nm, and the Mo layers occupied about half of the period (~9 and ~19 nm, respectively). The minimum concentration of silicon atoms in the middle of the Mo layers for both samples was approximately the same and exceeded 10 at.%.

Based on the above findings, we concluded that the most probable impurity in the Mo layers is Si. This is due to the fact that, firstly, during deposition there is an interaction between Mo and Si layers resulting in the formation of silicide interlayers [14]. It is worth noting, that these interlayers are formed in MXMs obtained not only by sputtering but also by evaporating [20], in which the energies of the deposited atoms are smaller by an order of magnitude. Secondly, thin Mo layers (t_{Mo}<2 nm) are amorphous [5], due to the presence of excessive Si atoms; and as the thickness of Mo layers increases, the Si content is reduced and Mo layers crystallize at certain thickness (t_{Mo}>2.2 nm). Thirdly, C, N, and O impurities form interstitial phases in c-Mo, which lead to an increase in the Mo lattice parameter [21, 22] rather than a decrease. Taking into account all these considerations, we can conclude that the amount of carbon, nitrogen and oxygen in Mo layers should be small, and their content in the first approximation can be neglected. Therefore, the main impurity in Mo layers can be only Si atoms.

It is known that the influence of impurities on the lattice parameter can be described by Vegard's law. Using the literature data for the dependence of the Mo lattice parameter on the Si content [23], we estimated the concentration of Si in Mo layers fabricated at different p_{Ar}. The obtained values are presented in Fig. 2. As can be seen from the figure, the maximum Si content is C_{Si}~4 %. The Si concentration changes little up to p_{Ar}~2 mTorr: it is constant for the "7 nm" series, while it decreases slightly from ~4 to ~3.5% for the "14 nm" series. Beginning from 2…2.2 mTorr, C_{Si} in the Mo layers of both series starts decreasing markedly, and at p~4 mTorr it is ~2.8 % for the "7 nm" series and almost zero for the "14 nm" series.

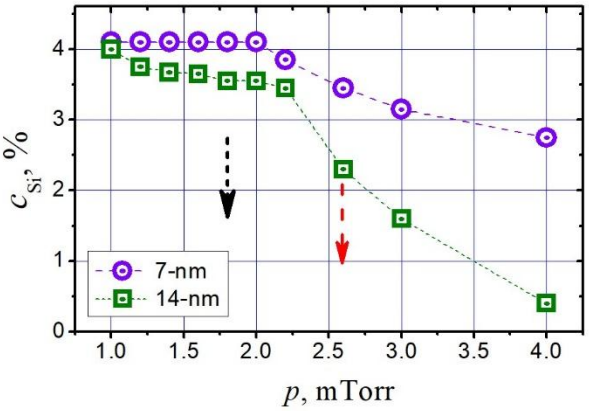

Fig. 2. Silicon concentration in Mo layers as a function of p_{Ar}. The arrow on the left indicates the pressure at which the free path length (FPL) of Mo atoms is equal to the distance between the magnetron etching zone and the center of the substrate; the arrow on the right – FPL is half the distance between the magnetron and the substrate

According to the equilibrium state diagram for the Mo-Si system, the limiting solubility of Si in Mo reaches 5% at the peritectic temperature (~2025 °C) [24]. Although in this work, MXMs are obtained at substrate temperature not more than ~100 °C, where the solubility of Si does not exceed 1 %, the solubility of Si may increase due to the defectivity of Mo crystals. In addition, thin Mo layers can be considered as a quenched state of matter, which carries the property of high-temperature state, so C_{Si}>1 % concentration can be expected in Mo layers. Molybdenum atoms are not soluble in Si layers.

We suppose that the data obtained for C_{Si} in [19] are overestimated and are a peculiarity of the technique used. Thus, the substance blown off the walls of the formed crater can lead to an overestimation of the content for a particular element, for example, silicon. In addition, argon ions used for etching can "knock" Si atoms into Mo layers or lead to heating the MXM surface, which promotes Si atom diffusion. The data obtained in this work also indicate that. Although Vegard's law is indirect method, it provides more reliable data without destroying the sample or introducing artifacts.

The presence of Si atoms in the Mo layers negatively affects the efficiency of multilayer mirrors, since the density of metal layers drops. Thus, if we take the tabulated densities of substances, the presence of 4 at.% silicon should lead to a decrease in the density of molybdenum from 10.218 to 9.818 g/cm^3, i.e. by 4%. Model calculations show that at the operating wavelength (λ~13.5 nm), the reflectivity of Mo/Si

MXM at normal incidence will decrease by ~1 % with such changes. Although this decrease is small, in X-ray lithography with a 9-mirror configuration, the loss would already be ~10%. In other words, increasing p_{Ar} can improve the efficiency of Mo/Si MXMs by reducing the Si content in Mo layers.

2.3. ESTIMATION OF DIFFUSION PARAMETERS

The presence of Si in Mo layers allows us to clarify the growth model of metal layers during deposition. First, amorphous silicide interlayers may be formed due to the high energy of Mo atoms deposited on Si layers, condensation energy, and due to the bombardment of the growing film surface by neutral Ar atoms reflected from the Mo target. At the Mo-on-Si interface, their formation occurs predominantly by ballistic mechanism [25].

At the second stage, when the energy of Mo atoms deposited on the formed silicide layers becomes insufficient to support the silicide formation, their energy is mainly spent on heating the silicide interlayers. This leads to the diffusion of Si atoms through the silicide into the growing Mo layers, since Si is a preferential diffusant in the Mo-Si system. It should be noted that silicide formation is an exothermic process [26], and the energy released during this process also contributes both to the increase in the thickness of silicide interlayers due to reaction diffusion and to the diffusion of Si atoms through the interlayer into the growing Mo layers. Silicon present in the growing Mo layers stabilizes their amorphous state when its concentration is higher than the limiting solubility of Si in Mo (C_{Si}>7%) [5, 27].

The third stage: as the thickness of Mo layers deposited on α-Mo layers increases, the Si concentration in them is reduced (due to diffusion of Si from the α-Mo layers). When C_{Si} becomes less than the solubility limit, the Mo layers crystallize [5]. The average Si concentrations in Mo for different Mo/Si MXMs are shown in Fig. 2.

Thus, during the deposition of Mo atoms on formed silicide interlayers, two processes are observed that are generally controlled by diffusion: 1) transport of Si atoms through the formed silicide into the adjacent α-Mo layers; and 2) diffusion of Si atoms from the regions adjacent to silicide α-Mo layers to the entire depth of the deposited Mo layers. The procedures used to estimate diffusion coefficients and activation energies for both processes are described below.

Earlier [28] it was found that at pressure p~1.8 mTorr a decrease in the scale of interlayer mixing with a contraction of silicide interlayers is observed. At this pressure, the free path length (FPL) of sputtered Mo atoms becomes comparable to the distance from the magnetron to the substrate. As can be seen from Fig. 2, at this pressure (vertical arrow on the left) the concentration of Si atoms in Mo layers changes little. The trend of decreasing C_{Si} starts to appear at higher pressures, namely at p_{Ar}>2.2 mTorr (arrow on the right). In this case, the distance from the magnetron to the substrate corresponds to two FPLs. The concentration of Si atoms for the "14 nm" series samples drops to almost zero at p_{Ar}~4 mTorr, when sputtered Mo atoms can collide three times with argon atoms on their way to the substrate.

Assuming that the Si content is averaged over the entire thickness of the Mo layers, we, knowing the thickness of the metal layers, calculated the amount of Si atoms dissolved in the Mo layers. For this purpose, we used tabulated values of the densities. If we express this amount of silicon in the effective thickness t_{Si}*, we can show that its value is expressed by the following formula:

$$t_{Si}^* = [\rho_{Mo} \times A_{Si}/(\rho_{Si} \times A_{Mo})] \times [C_{Si}/C_{Mo}] \times t_{Mo}, \quad (1)$$

with ρ being the density of the substance, A being the atomic weight, and C being the atomic concentration. Calculations show that t_{Si}* for samples of both series lie in the range of 0.02…0.3 nm. If we consider this Si as atoms constituting the flow of matter, J, from the Si layer to the Mo layer, then in accordance with Fick's first law [J=-D×(dC/dX] we can estimate the diffusion coefficient of Si, D_{Si}, into the Mo layers through the bottom interface (Mo-on-Si) by the formula:

$$D_{Si} = -J_{Si}/(dC_{Si}/dX), \quad (2)$$

with C_{Si} is the atomic concentration of Si in a unit volume, dC_{Si}/dX is the concentration gradient of Si atoms at the Mo-on-Si interface. The value of "X" is actually determined by the thickness of the silicide interlayer at this interface, which can be easily estimated from the volume shrinkage in the Mo/Si MXMs that we monitored for each sample. The atomic concentration of Si in the Mo layers is taken from Fig. 2, and that in the Si layer is tabulated. Knowing all the components of formula (2), we calculated the diffusion coefficients for all pressures and presented them in Fig. 3,a as light circles ("7 nm" series) and dark squares ("14 nm" series). The diffusion coefficients exceed $2.5 \cdot 10^{-20}$ m^2/s for small p_{Ar}. At pressure p_{Ar}~1.8 mTorr they start to decrease and at large pressures ($p_{Ar} \geq 3$ mTorr) they are ~10^{-21} m^2/s and lower. It is interesting to note the following fact: despite the absence of any features on the $C_{Si}=f(p_{Ar})$ dependence at pressure p_{Ar}~1.8 mTorr (see Fig. 2), the diffusion coefficients D_{Si} at this pressure begin to decrease, i.e. D_{Si} is sensitive to the change in the energy of the deposited atoms (see Fig. 3,a). A noticeable change in the D_{Si} drop rate at p_{Ar}>2.2 mTorr (Fig. 4) correlates with the onset of C_{Si} decrease (see Fig. 2).

On the other hand, we can also estimate the diffusion coefficients (D_{If}) of Si from the adjacent to silicide regions into the crystalline Mo layers. It has been previously shown that Mo layers in Mo/Si MXMs deposited at a pressure of p_{Ar}~1 mTorr are amorphous up to a thickness of t_{Mo}~2 nm [5, 29]. In our case, the nominal Mo layer thicknesses were in the range of 2.3…3.2 nm for the "7 nm" series and 3.6…5.3 nm for the "14 nm" series, i.e., beyond the amorphization thickness. If the Si content decreases with Mo layer thickness, it means that there is some initial layer of α-Mo in which the main amount of Si is concentrated. During further growth and crystallization of Mo layers, this layer is the main supplier of silicon. In other words,

it is precisely because of the limited Si source that C_{Si} decreases with both the thickness of the Mo layers and p_{Ar}. In our opinion, the thickness of the α-Mo layer and, accordingly, the amount of Si in it should decrease with increasing pressure, since the energy of Mo atoms hitting the substrate as a result of collisions with Ar atoms decreases. Considering that the thickness of the α-Mo layer is less than the total thickness of the deposited layer, we used the formula describing the diffusion profile of Si atoms distribution in the thin-film source approximation [30]:

$$C_{Si}(x,\tau)=C_0\times\exp[-x^2/(4D_{If}\tau)], \quad (3)$$

with $C_{Si}(x,\tau)$ is the concentration profile of Si atoms along the spatial coordinate "x" and time coordinate "τ", C_0 is the concentration of Si atoms in the thin film source, D_{If} is the diffusivity of Si atoms into the Mo layer.

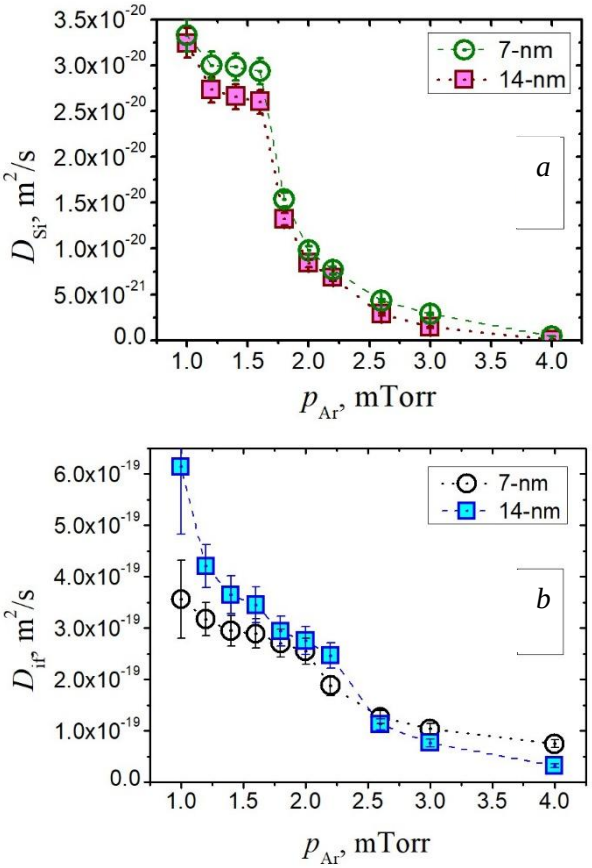

Fig. 3. Diffusion coefficients (D_{Si}) of Si through the silicide interlayer at the Mo-on-Si interface (a). Silicon diffusion coefficients (D_{If}) from the interface region (Mo-on-Si interface) into Mo crystal layers (b)

Using formula (3), we estimated the diffusion coefficient having two points: the first one with coordinate $C_{Si}(x=0)$=5 at.%, corresponding to the maximum concentration of dissolved Si in the Mo layers; and the second one at the center of the Mo layer, i.e., $C_{Si}(x=t_{Mo}/2)$, with concentrations shown in Fig. 2. Since the deposition time of all Mo layers was the same in each series and different in different series, we evaluated the diffusion coefficients for each series separately. In calculating D_{If}, we used the total deposition time minus the Mo deposition time spent to form silicide interlayers. The results of the calculations are presented in Fig. 3,b. Here we see that the diffusion coefficients immediately begin to fall with increasing pressure, their fall slows down by p_{Ar}~2 mTorr, and then at p_{Ar}>2.2 mTorr the next stage of their decrease is observed. The decrease in the diffusion coefficient at the first site (p_{Ar}<2 mTorr) is probably due to a 30% drop in the energy of Ar atoms reflected from the Mo target and irradiating the growing Mo film. Other deposition parameters, as shown by calculations using the SRIM program [30] (number of reflected Ar atoms, Mo atom energies), change little. Since the errors in the estimation of diffusion coefficients at the first site are large, it is possible that the change in diffusion coefficients here is smaller and does not exceed ~$1.8\cdot10^{-19}$ m^2/s (on the graph the difference is ~$3.4\cdot10^{-19}$ m^2/s). The second drop region is most likely related to the energy drop of sputtered Mo atoms colliding with Ar atoms on their way to the substrate.

When estimating the diffusion coefficients across c-Mo layers, we assume the maximum amount of Si in α-Mo layers based on the maximum solubility of Si in the Mo-Si system [24]. However, if the solubility of Si in the thin α-Mo film is higher, the diffusion coefficients may be different. We made additional calculations of the diffusion coefficients D_{If} for the case when the maximum concentration of Si in Mo is 7 at.%. On average, we obtain diffusion coefficients 2 times smaller than for the case of 5 at.%. This finding can be explained by the fact that the Si concentration gradient in Mo layers for $C_{Si}(0,0)$ = 7% becomes higher, so lower diffusion coefficients are required to equalize this gradient.

Amorphous Mo/Si MXMs are characterized by the presence of silicide interlayers up to 1…1.2 nm thick at both interlayers [29]. In MXMs with crystal Mo layers, the thickness of the top interlayer (Si-on-Mo interface) is approximately 2 times less compared to that of the bottom silicide interlayer. This fact also indicates greater Si diffusivity on the side of the bottom interlayer. The calculations confirm the experimental observation: even taking into account that the deposition rate of Si layers is about one and a half times higher with respect to Mo, the predominant energy with deposited atoms falls on the bottom interlayer (Mo-on-Si). The situation does not change even at p_{Ar}~4 mTorr, despite the fact that the energies of the sputtered atoms decrease by about an order of magnitude. Thus, it can be concluded that Si diffusing into Mo layers comes mainly from the bottom interface (Mo-on-Si). Therefore, although some amount of Si can also enter Mo layers through the top interface (Si-on-Mo), we neglected this amount in these estimates.

It is interesting to note that the diffusion coefficients through the silicide layer (see Fig. 3,a) are on average at least an order of magnitude lower compared to the diffusion within the Mo layers (see Fig. 3,b). To establish the reason for this difference, we estimated the activation energies of both processes from the available diffusion coefficients. We used the annealing data of Mo/Si MXMs [31]. According to these data, the diffusion coefficient for the Mo-on-Si interface is:

$$D=6\times10^{-5}\times\exp[-2.3eV/(kT)]\ m^2/s \quad (4)$$

(k is Boltzmann constant, T is absolute temperature).

The temperature on the surface of the coating can be estimated from the thickness of the silicide layer through volumetric shrinkage in the Mo/Si MXM, which is known to us, since we controlled the deposition rates of the components at all Ar pressures. Shrinkage, which is equal to the difference between the nominal and experimental MXM periods, is observed for all samples. Knowing the shrinkage value, it is possible to calculate the thickness of the disilicide layer (t_{MoSi2}) in each sample. Then we determined the diffusion coefficient of Si according to the formula $D=(t_{MoSi2})^2/\tau_{MoSi2}$ [9], with τ_{MoSi2} is the formation time of the disilicide layer, i.e. the deposition time of the Mo layer involved in the formation of the bottom disilicide layers. Substituting the obtained D values into formula (4) we established that the temperatures on the deposited surface can reach values from ~720 K (~450 °C at p_{Ar}~4 mTorr) to ~870 K (~600 °C at p_{Ar}~1 mTorr). Similar values of film surface temperatures were obtained during the deposition of chromium (T<800 K) and copper (T<1300 K) [32] coatings.

Arrhenius plots for both diffusion processes are shown in Fig. 4. The slope angle tangents for the straight lines drawn through the corresponding experimental points give the activation energies for each of the processes. For the "7 nm" series, the activation energy of the Si diffusion process through the silicide layer is (1.96±0.10) eV, and for the "14 nm" series it is (2.19±0.13) eV, or an average of (2.08±0.13) eV. This value is slightly less than the activation energy of silicide formation during annealing [31], and this is most likely due to a decrease in the free volume in films during annealing [33]. It is interesting to note that the activation energy of self-diffusion of Si atoms over Mo disilicide is ~2.1 eV [34, 35], i.e. in our case and in the case of annealing, we deal with the diffusion of silicon atoms through the formed disilicide interlayer.

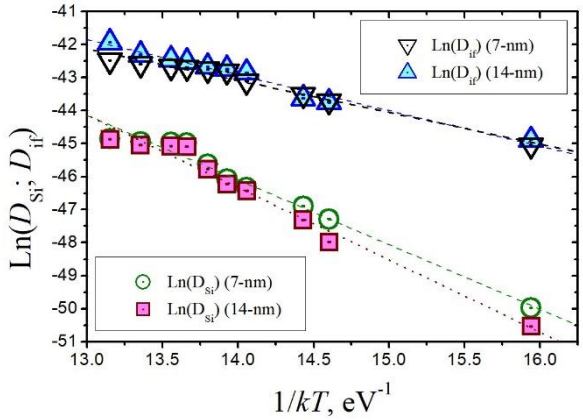

Fig. 4. Arrhenius plots for Si diffusion through silicide interlayers (Mo-on-Si interface) (squares and circles) and through molybdenum crystalline layers (triangles)

In the case of diffusion of Si atoms over Mo layers (see triangles in Fig. 4), the average activation energy is (1.02±0.07) eV, i.e. almost half as much as for the process of Si diffusion through the disilicide layer. This low activation energy may be due to diffusion along Mo crystallite boundaries [23]. Despite the fact that Mo layers are textured and individual Mo crystallites occupy the entire space between two silicide interlayers [15], they have an acicular shape; have structural defects and may contain quite a lot of clusters [36].

We also estimated the activation energy for Si atoms into the Mo layers for the case when the near-boundary α-Mo layer initially contains 7 at.% Si. This value is (0.74±0.21) eV, which is inferior to the data obtained above. The lower activation energy can only indicate an acceleration of the diffusion process, which indicates that the Mo layers are defective. On the other hand, a higher error in determining the activation energy shows that the estimates made above are closer to the true ones.

Thus, the diffusion of Si atoms into Mo layers through the Mo-on-Si interface can be divided into three stages: 1) reactive diffusion with the formation of silicide interlayers, 2) diffusion of Si atoms through silicide interlayers and saturation of near-silicide Mo layers with silicon, and 3) diffusion of silicon from amorphous near-silicide Mo layers into crystalline Mo.

CONCLUSIONS

Using X-ray tensometry ($\sin^2\psi$-method), X-ray reflectometry and X-ray diffractometry (λ=0.154 nm), the diffusion processes in crystal Mo layers during the deposition of Mo/Si multilayer X-ray mirrors (periods: 6…16 nm; $2.3<t_{Mo}<5.9$ nm) fabricated by magnetron sputtering in Ar at pressures of p_{Ar}=1…4 mTorr have been studied. The above results lead to the following conclusions:

1. The lattice parameters of the c-Mo layers in the unstressed state are below the tabular value (0.3147 nm) and increase with p_{Ar} from 0.3139 to 0.3147 nm. The main reason is the presence of dissolved Si atoms, which have a smaller atomic radius. The Si content decreases with increasing p_{Ar}. At p_{Ar}~4 mTorr, the lattice parameter of the c-Mo layers approaches the tabulated value.

2. The concentration of Si atoms in c-Mo layers, estimated by Vegard's law, do not exceed 4 at.% (p_{Ar}=1 mTorr), and gradually decrease with increasing pressure. A noticeable decrease of Si atoms in the c-Mo layers is observed at p_{Ar}>2.6 mTorr, when the mean free path length of Mo atoms in Ar medium is half the magnetron-substrate distance.

3. The growth model of Mo layers on amorphous Si layers has been refined. During the deposition of Mo atoms on the formed silicide interlayers, two diffusion-controlled processes are observed: 1) the transport of Si atoms through the silicide into the adjacent α-Mo layers; 2) the diffusion of Si atoms from these regions to the full depth of the deposited Mo layers.

4. The diffusivity of Si atoms through the silicide layer (Mo-on-Si interface) and into the c-Mo layers differ by at least an order of magnitude and average ~$1.5\cdot10^{-20}$ and ~$2.5\cdot10^{-19}$ m^2/s, respectively. The activation energies for these processes are (2.08±0.13) and (1.05±0.07) eV, respectively. In the first case, it indicates the process of silicon self-diffusion through the silicide layer; in the second case, it points to the Si atom diffusion along the boundaries of Mo crystallites.

5. The presence of Si in Mo layers can reduce the reflectivity of multilayer Mo/Si X-ray mirrors at the

working wavelength (λ=13.6 nm) by about 1% and decrease the efficiency of the lithographic system as a whole, where these mirrors are used.

ACKNOWLEDGEMENTS

Y. P. P. is acknowledged to ISKCON for improving the realization with regard to the place of this work.

REFERENCES

1. E. Louis, A.E. Yakshin, P.C. Goerts, S. Oestreich, R. Stuik, E.L. G. Maas, M.J.H. Kessels, F. Bijkerk, M. Haidl, S. Muellender, M. Mertin, D. Schmitz, F. Scholze, G. Ulm. Progress in Mo/Si multilayer coating technology for EUVL optics // *Proc. SPIE*. 2000, v. 3997, p. 406-411.

2. S. Bajt, J.B. Alameda, T.W. Barbee, W.M. Clift, J.A. Folta, B.B. Kaufmann, E.A. Spiller. Improved reflectance and stability of Mo-Si multilayers // *Opt. Eng.* 2002, v. 41, № 8, p. 1797–1804.

3. S. Braun, P. Gawlitza, M. Menzel, S. Schädlich, A. Leson. High Precision Multilayer Coatings and Reflectometry for EUV Lithography Optics // *AIP Conf. Proc.* 2006, v. 879, p. 1482-1485.

4. Е.Н. Зубарев, В.В. Кондратенко, О.В. Польцева, В.А. Севрюкова, А.И. Федоренко и С.А. Юлин. Межфазные перемешанные зоны в сверхрешетках Mo-Si // *Металлофиз. новейшие технол.* 1997, т. 19, с. 56-63.

5. S. Bajt, D.G. Stearns, P.A. Kearney. Investigation of the amorphous-to-crystalline transition in Mo/Si multilayers // *J. Appl. Phys.* 2001, v. 92, № 2, p. 1017-1025.

6. S.S. Andreev, S.V. Gaponov, S.A. Gusev, M.N. Haidl, E.B. Kluenkov, K.A. Prokhorov, N.I. Polushkin, E.N. Sadova, N.N. Salashchenko, L.A. Suslov, S.Yu. Zuev. The microstructure and X-ray reflectivity of Mo/Si multilayers // *Thin Solid Films.* 2002, v. 415, p. 123-132.

7. E.N. Zubarev, V.V. Kondratenko, Yu.P. Pershyn, V.A. Sevryukova. Growth and crystallization of molybdenum layers on amorphous silicon // *Thin Solid Films.* 2011, v. 520, p. 314-319.

8. A.K. Petford-Long, M.B. Stearns, C.H. Chang, S.R. Nutt, D.G. Stearns, N.M. Ceglio, A.M. Hawryluk. High resolution electron microscopy study of x-ray multilayer structures // *J. Appl. Phys.* 1987, v. 61, № 4, p. 1422-1428.

9. C. Largeron, E. Quesnel, J. Thibault. Interface growth mechanism in ion beam sputtering-deposited Mo/Si multilayers // *Phil. Mag.* 2006, v. 86, № 19, p. 2865-2879.

10. D.G. Stearns, R.S. Rosen, S.P. Vernon. High-performance multilayer mirrors for soft x-ray projection lithography // *Proc. SPIE.* 1991, v. 1547, p. 2-13.

11. P. Boher, Ph. Houdy, and L. Ilennet, M. Küline, P. Muller, J.P. Frontier, P. Trouslard, C. Senillou, J.C. Joud, P. Ruterana. Structural characteristics and performances of rf-sputtered Mo/Si and Co/Si multilayers for soft X-ray optics // *Proc. SPIE.* 1991, v. 1547, p. 21-38.

12. J.M. Slaughter, A. Shapiro, P.A. Kearney, C.M. Falco. Growth of molybdenum on silicon: Structure and interface formation // *Phys. Rev. B.* 1991, v. 44, № 8, p. 3854-3863.

13. K. Holloway, K.B. Do, R. Sinclair. Interfacial reactions on annealing molybdenum-silicon multilayers // *J. Appl. Phys.* 1989, v. 65, № 2, p. 474-480.

14. R.S. Rosen, D. Stephen, P. Vernon, G. Stearns, M.A. Viliardos, M.E. Kassner, Y. Cheng. Silicide layer growth rates in Mo/Si multilayers // *Appl. Opt.* 1993, v. 32, № 34, p. 6975-6980.

15. E.N. Zubarev, A.V. Zhurba, V.V. Kondratenko, V.I. Pinegyn, V.A. Sevryukova, S.A. Yulin, T. Feigl, N. Kaiser. The structure, diffusion and phase formation in Mo/Si multilayers with stressed Mo layers // *Thin Solid Films.* 2007, v. 515, p. 7011-7019.

16. Е.Н. Зубарев. Ионно-лучевое перемешивание в слоистых системах // *Успехи физ. мет.* 2010, т. 11, с. 175-207.

17. Л.И. Гладких, С.В. Малыхин, А.Т. Пугачев. *Дифракционные методы анализа внутренних напряжений. Теория и эксперимент*. Харьков: НТУ «ХПИ», 2006, 304 с.

18. V.I. Pinegyn, E.N. Zubarev, V.V. Kondratenko, V.A. Sevryukova, S.A. Yulin, T. Feigl, N. Kaiser. Structure and stressed state of molybdenum layers in Mo/Si multilayers // *Thin Solid Films*. 2008, v. 16, p. 2973-2980.

19. Ю.П. Першин, В.А. Севрюкова, Е.Н. Зубарев, А.С. Оберемок, В.П. Мельник, Б.Н. Романюк, В.Г. Попов, П.М. Литвин. Исследование границ раздела фаз в периодических многослойных структурах Mo/Si с использованием метода масс-спектрометрии нейтральных частиц // *Металлофиз. новейшие технол.* 2013, т. 35, № 13, с. 1617-1627.

20. V.I.T.A. de Rooij-Lohmann, A.E. Yakshin, E. Zoethout, J. Verhoeven, F. Bijkerk. Reduction of interlayer thickness by low-temperature deposition of Mo/Si multilayer mirrors for X-ray reflection // *Appl. Surf. Sci.* 2011, v. 257, № 14, с. 6251-6255.

21. Х. Дж. Гольдшмидт. *Сплавы внедрения*. М.: «Мир», 1971, т. 1-2, 888 с.

22. Е. Фромм, Е. Гебхардт. *Газы и углерод в металлах*, М.: «Металлургия», 1980, 712 с.

23. D. Sturm, M. Heilmaier, J.H. Schneibel, P. Jehanno, B. Skrotzki, H. Saage. The influence of silicon on the strength and fracture toughness of molybdenum // *Materials Science and Engineering*. 2007, v. A463, p. 107-114.

24. Н.П. Лякишев. *Диаграммы состояния двойных металлических систем*. М: «Машиностроение», 2001, т. 3, 872 с.

25. W.L. Morgan and D.B. Boercker. Simulating growth of Mo/Si multilayers // *Appl. Phys. Lett.* 1991, v. 69, № 10, p. 1176-1178.

26. Ш. Мьюрарка. *Силициды для СБИС*. М.: «Мир», 1986, 176 с.

27. P.J. Desre and A.R. Yavari. Suppression of Crystal Nucleation in Amorphous Layers with Sharp Concentration Gradients // *Phys. Rev. Lett.* 1990, v. 64, № 13, p. 1533-1536.

28. Y.P. Pershyn, E.M. Gullikson, V.V. Kondratenko, V.V. Mamon, S.A. Reutskaya, D.L. Voronov, E.N. Zubarev, I.A. Artyukov A.V. Vinogradov. Effect of working gas pressure on interlayer mixing in

magnetron-deposited Mo/Si multilayers // *Opt. Eng.* 2013, v. 52, № 9, p. 095104 (10 pages).

29. S. Yulin, T. Feigl, T. Kuhlmann, N. Kaiser, A.I. Fedorenko, V.V. Kondratenko, O.V. Poltseva, V.A. Sevryukova, A.Yu. Zolotaryov, E.N. Zubarev. Interlayer transition zones in Mo/Si superlattices // *J. Appl. Phys.* 2002, v. 92, № 3, p. 1216-1220.

30. M. Salamon, H. Mehrer, Diffusion in molybdenum disilicide // *Z. Metallkd.* 2005, v. 96, № 8, p. 833-842.

31. Е.Н. Зубарев. Реакционная диффузия в наноразмерных слоистых системах металл/кремний // *Успехи физ. наук.* 2001, т. 181, № 5, с. 491-520.

32. L.R. Shaginyan, J.G. Han, V.R. Shaginyan, J. Musil. Evolution of film temperature during magnetron sputtering // *J. Vac. Sci. Technol. A.* 2006, v. 24, № 4, p. 1083-1090.

33. O.B. Loopstra, E.R. van Snek, T.H. de Keijser, E.J. Mittemeijer. Stress and Volume Changes in Amorphous Mo/Si Multilayers on Annealing // *Materials Science Forum.* 1994, v. 154, p. 55-68.

34. M. Salamon, A. Strohm, T. Voss, P. Laitinen, I. Riihimäki, S. Divinski, W. Frank. Self-diffusion of silicon in molybdenum disilicide // *Phil. Mag.* 2004, v. 84, № 8, p. 737-756.

35. I.V. Belova, H. Mehrer, G.E. Murch. Diffusion correlation effects of molybdenum and silicon in molybdenum disilicide // *Phil. Mag.* 2011, v. 91, № 28, p. 3727-3743.

36. E.N. Zubarev, V.V. Kondratenko, Yu.P. Pershyn, V.A. Sevryukova. Growth and crystallization of molybdenum layers on amorphous silicon // *Thin Solid Films.* 2011, v. 520, p. 314-319.

Article received 25.09.2024

ДИФУЗІЙНІ ПРОЦЕСИ В МЕТАЛЕВИХ ШАРАХ БАГАТОШАРОВИХ РЕНТГЕНІВСЬКИХ ДЗЕРКАЛ Mo/Si ПІД ЧАС ОСАДЖЕННЯ

Ю.П. Першин, В.С. Чумак, О.Ю. Девізенко, Є.М. Зубарєв, В.А. Севрюкова, Н.О. Кириллова, Л.Є. Конотопський

Методами малокутової рефлектометрії, рентгенівської дифрактометрії та рентгенівської тензометрії (λ=0,154 нм) досліджено структуру шарів Mo у багатошарових рентгенівських дзеркалах (БРД) Mo/Si, виготовлених магнетронним напиленням як функцію тиску Ar у діапазоні 1…4 мТорр. Було виготовлено дві серії зразків з періодами приблизно 7 і 14 нм. У всіх БРД шари Mo були кристалічними (c-Mo), а шари Si – аморфними. У середньому параметр ґратки a_0 у ненапруженому стані менший для зразків серії 7 нм, ніж для – серії 14 нм. Він зростає з тиском Ar, наближаючись до табличного. Оцінено вміст кремнію в шарах c-Mo. Визначено коефіцієнти дифузії атомів кремнію в шари c-Mo та їх енергії активації. Запропоновано механізми дифузії.